Inorganic Chemistry

Article

pubs.acs.org/IC

A Sterically Demanding Iminopyridine Ligand Affords Redox-Active Complexes of Aluminum(III) and Gallium(III)

Thomas W. Myers and Louise A. Berben*

Department of Chemistry, University of California, Davis, California 95616, United States

Supporting Information

ABSTRACT: The combination of an electrophilic metal center with a redox active ligand set has the potential to provide reactivity unique from transition metal redox chemistry. In this report, substituted iminopyridine complexes containing monoanionic and dianionic $^{Me}IP_{Mes}$ ligands have been characterized structurally and electronically. Green ($^{Me}IP_{Mes}{}^{-}$)$AlCl_2$ (**1**), ($^{Me}IP_{Mes}{}^{-}$)$AlMe_2$ (**2**), and ($^{Me}IP_{Mes}{}^{-}$)$GaCl_2$ (**5**) have a doublet spin state which results from the anion radical form of $^{Me}IP_{Mes}$. Purple ($^{Me}IP_{Mes}{}^{2-}$)$AlCl(OEt_2)$ (**3**), ($^{Me}IP_{Mes}{}^{2-}$)$AlMe(OEt_2)$ (**4**), and ($^{Me}IP_{Mes}{}^{2-}$)$GaCl(OEt_2)$ (**6**) are each diamagnetic. We have also investigated the solvent dependence of the decomposition of the $^{Me}IP_{Mes}$ anion radical. Complexes **1** and **2** can be obtained from benzene and hexanes whereas the use of ether solvents results in the formation of undesirable ($^{CH2}IP_{Mes}{}^{-}$)$AlCl_2$ (**1a**) and ($^{CH2}IP_{Mes}{}^{-}$)$AlCl_2$ (**2a**) formed by loss of a hydrogen atom from the $^{Me}IP_{Mes}{}^{-}$ ligand. Electrochemical measurements indicate that **1**, **2**, and **5** are redox active.

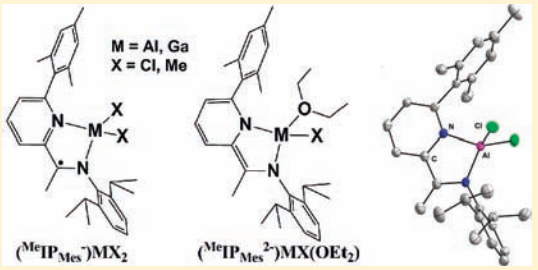

INTRODUCTION

Electrophilic transition metal complexes of redox-active ligands have been studied by Heyduk and co-workers. These studies focused mostly on zirconium and tantalum and, in particular a zirconium complex which can reductively eliminate biphenyl was investigated.[1] In the present work we make use of a substituted iminopyridine ligand in conjunction with aluminum(III) and gallium(III). Previous work, by both Westerhausen and co-workers, and by Wieghardt and co-workers, has demonstrated that the iminopyridine ligand (Chart 1) can behave as a redox active ligand and can stabilize magnesium and transition metal complexes, respectively.[2] These previous reports incorporated IP ligands in the neutral, singly reduced, and doubly reduced oxidation states.[2a,3] In general, highly electrophilic group 13 metal ions are not redox active and to investigate concurrent electrophilic and redox reactivity we are investigating aluminum(III) and gallium(III) complexes of redox active ligands.

We have previously reported the synthesis of aluminum(III) complexes with the redox-active iminopyridine ligand, 2,6-bis(isopropyl)-*N*-(2-pyridinylmethylene)phenylamine (henceforth denoted by IP, Chart 1).[4] In that work, the redox chemistry and electronic structure of complexes which have coordination numbers of four or five were investigated: $(IP^{n-})_2Al$ or $(IP^{n-})_2Al{-}X$ (where X = monodentate ligand). The five-coordinate complexes that we reported were neutral or anionic, and the four-coordinate complexes were anionic. In the present work we have lowered the coordination number of the metal center to increase the electrophilicity of the complexes.

Aryl-substituted iminopyridine ligands ($^{Me}IP_{Ph}$) have previously been employed as sterically demanding ligands in the chemistry of transition metal ions. For example, as the ancillary ligand in the chemistry of the copper(I) complex, ($^{Me}IP_{Ph}$)Cu-($O_2CC(O)Ph$), the large size of ^{Me}IP-Ph provided a platform to position an aryl ring in close proximity to the site of putative Cu−O bond formation when ($^{Me}IP_{Ph}$)Cu(O_2CC-(O)Ph) reacts with dioxygen.[5] Subsequent to reaction with dioxygen, hydroxylation of the well-positioned aryl ring in $^{Me}IP_{Ph}$ demonstrated the strong oxidizing power of a proposed Cu(III)-oxo functional group. In a further example of $^{Me}IP_{Ph}$ chemistry, formation of tetrahedral cobalt complexes was investigated and yielded ($^{Me}IP_{Ph}$)$CoCl_2$.[6] It was shown that this complex and its derivatives, in conjunction with methylaluminumoxide (MAO), are active for the polymerization of ethylene. The turnover frequencies (TOF) for the polymerization reactions were shown to be 2 orders of magnitude faster than had been reported for the square planar complexes of cobalt formed from the analogous but tridentate 2,6-bis(imino)-pyridine ligand ($^{Me}I_2P$): ($^{Me}I_2P$)CoCl.[7] In all cases that we are aware of, the bulky $^{Me}IP_{Ph}$ ligand participates as a neutral and redox-innocent ligand.

In the foregoing report, we have shown that $^{Me}IP_{Mes}$ can behave as a redox-active ligand in the same way that we and others have previously employed the less bulky, unsubstituted iminopyridine ligand (IP).[4] Because of the steric bulk of the $^{Me}IP_{Mes}$ ligand, these complexes contain only one $^{Me}IP_{Mes}$ ligand each, and can be described by the general formulation ($^{Me}IP_{Mes}{}^{n-}$)$Al{-}X_{3-n}$ (X = Cl, Me, n = 1, 2). We have also investigated the formation of gallium(III) complexes with $^{Me}IP_{Mes}{}^{n-}$. We demonstrate that tetrahedral complexes of aluminum(III) and gallium(III) can be isolated where the ($^{Me}IP_{Mes}$)

Received: August 8, 2011
Published: January 5, 2012

 © 2012 American Chemical Society dx.doi.org/10.1021/ic201729b | *Inorg. Chem.* 2012, 51, 1480−1488

Chart 1. Structures of Ligands Mentioned in the Text with Their Abbreviations

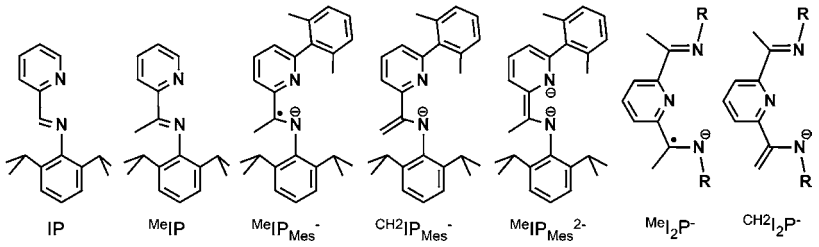

ligand is in the 1- or the 2- oxidation state. We have also found that reaction conditions must be carefully chosen to prevent decomposition pathways for the anion radical oxidation state of the ligand $^{Me}IP_{Mes}^{-}$, to afford $^{CH2}IP_{Mes}^{-}$ after loss of a hydrogen atom (Chart 1). The known one-electron reduced complexes of methyl-substituted iminopyridine (^{Me}IP) and bis(imino)pyridine ($^{Me}I_2P$) derivatives are also often reported in the alkene form ($^{CH2}IP^{-}$ and $^{CH2}I_2P^{-}$) and we show that this decomposition pathway can be circumvented by judicious choice of solvent. In the absence of decomposition pathways, aluminum and gallium complexes with doublet electronic states arise from the singly reduced ligands, while complexes of the doubly reduced ligands are diamagnetic.

RESULTS AND DISCUSSION

Synthesis of Aluminum and Gallium Complexes 1−6. Synthesis of aluminum and gallium complexes of the reduced $^{Me}IP_{Mes}$ employed sodium metal as a reductant because we had found this to be effective in our previous syntheses of $[(IP^{n-})_2Al]^{m-}$ complexes (Scheme 1).[4] In previous work, we proposed that the stability of the ligand radicals in $(IP^{-})_2AlCl$ was due at least in part, to exchange coupling through the aluminum center. In the present work we have found that the complexes of the form $(^{Me}IP_{Mes}^{-})AlX_2$ which contain only one ligand radical are indeed less stable, under some reaction conditions, than those we have previously isolated as diradical complexes. We found that the most successful method for synthesis of $(^{Me}IP_{Mes}^{-})AlCl_2$ (**1**), $(^{Me}IP_{Mes}^{-})AlMe_2$ (**2**), and $(^{Me}IP_{Mes}^{-})GaCl_2$ (**5**) employed benzene as reaction solvent and hexane for workup and crystallization. The ligand $^{Me}IP_{Mes}$ was initially reduced with 1 equiv of sodium metal in benzene after which time $AlCl_3$, $AlMe_2Cl$, or $GaCl_3$, respectively, were added as a solid. The resulting dark green products were purified and crystallized from hexane.

Scheme 1. Synthesis of Aluminum and Gallium Compounds

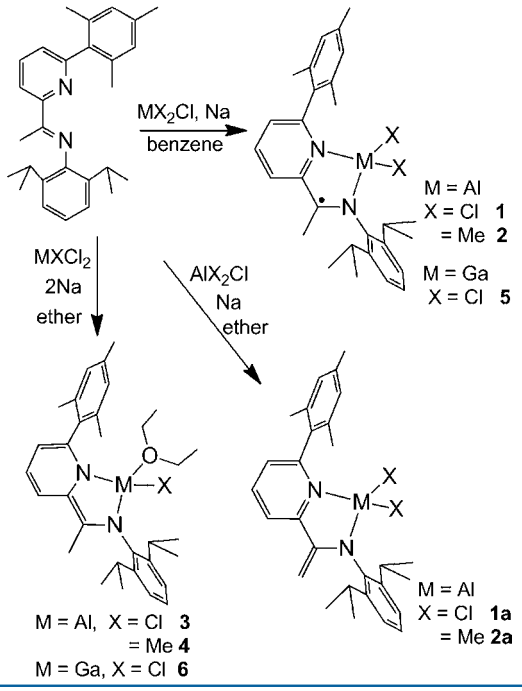

The formation of the aluminum(III) complexes was also investigated in alternate solvents. When ether is employed as the reaction solvent, the alkene products, $(^{CH2}IP_{Mes}^{-})AlCl_2$ (**1a**) and $(^{CH2}IP_{Mes}^{-})AlMe_2$ (**2a**), respectively, were obtained. (Chart 1, Scheme 1). The CH_2 alkene group in complexes **1a** and **2a** was identified by ^1H NMR spectroscopy and are observed as doublets at 4.10 and 4.73 in **1a** and at 3.90 and 4.68 in **2a**. In addition, the $C_{im}-C_{Me}$ bond lengths, observed crystallographically, are distinct for each of the ligand forms (vide infra). In some experiments, mixtures of **1**:**1a**, or **2**:**2a** were obtained, and the ratio of the products was dependent on reaction time and the solvents employed for the purification of the complexes. The same reactivity patterns were observed when we employed AlI_3 as the starting reagent in place of $AlCl_3$.

In the chemistry of methyl-substituted iminopyridine ligand (^{Me}IP) and methyl-substituted bis(imino)pyridine ligand ($^{Me}I_2P$) reported in the literature, both forms of the one electron reduced ligand that we report here are commonly observed. Therefore, understanding the conditions and that lead to formation of each of our ligand forms, $^{Me}IP_{Mes}^{-}$, and $^{CH2}IP_{Mes}^{-}$, may be of general interest. We have observed that complexes of the alkene ligand $^{CH2}IP_{Mes}^{-}$, **1a** and **2a**, are obtained when an ether is used as the reaction solvent for the reduction of the ligand with sodium metal. In an independent reaction of $^{Me}IP_{Mes}$ with sodium in ether, single crystals of $Na(^{CH2}IP_{Mes}^{-})$ (**7**) were obtained which suggests that formation of the alkene occurs during ligand reduction and is independent of the reaction with the aluminum salt (Figure 1). The alkene nature of **7** was identified crystallographically, and the bond distances in the compound are discussed below.

The reduction chemistry of $^{Me}IP_{Mes}$ has not been previously studied. However, we have observed parallels with the corresponding $^{Me}I_2P$ chemistry reported in the literature. In addition, deprotonation of other potentially redox active ligands such as α-diimines,[8] α-iminoketones,[9] salens,[10] and others[11,12] has been reported by others. On the basis of the reported observations pertaining to $^{Me}I_2P$ and our own observations, we have been able to identify conditions under which the anion radical form of $^{Me}IP_{Mes}$ (or presumably $^{Me}I_2P$ or ^{Me}IP) can be obtained selectively (Chart 1).[13−16] A common theme in these reports,

dx.doi.org/10.1021/ic201729b | Inorg. Chem. 2012, 51, 1480−1488

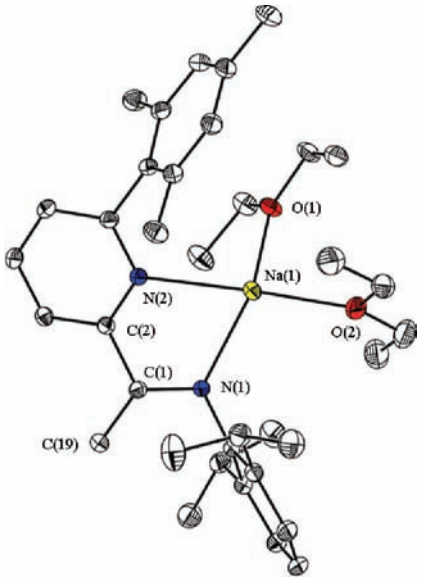

Figure 1. Solid state structure of **7**. Yellow, white, and blue ellipsoids represent Na, C, and N atoms, respectively; ellipsoids are shown at the 50% probability level. H atoms omitted.

and in our own observations, is that an ether solvent (usually tetrahydrofuran (THF) or diethylether) is used as the reaction solvent when complexes of ^{CH2}IP[17] and $^{CH2}I_2P$,[18] which are analogues of $^{CH2}IP_{Mes}^{-}$, are observed. In addition, reduction of the ligand prior to metal salt addition leads to decomposition of the anion radical to afford the alkene ligand form. Synthetic methods in which unreduced ligand, reductant, and metal salt are mixed concurrently lead more reliably to formation of he one-electron reduced anion radical form of the ligand analogous to $^{Me}IP_{Mes}^{-}$. The anion radical form of $^{Me}I_2P$ has also been accessed via transmetalation from an iron(II) complex to aluminum(III) in toluene,[19] and gallium complexes of $^{Me}I_2P^{-}$ can be accessed by reduction of the neutral ligand by GaI;[20] both of these situations are variations of a synthetic method in which concurrent addition of reductant and metal salt to the unreduced ligand is employed.

Although less common, successful formation of the anion radical form of the I_2P ligand by reduction of the neutral ligand complex has been demonstrated. Chirik and co-workers reported that ($^{Me}I_2P$)$CoCl_2$ can be reduced to the radical anion ($^{Me}I_2P^{-}$)CoCl in toluene by Zn metal, and also by strong bases such as alkyl lithium reagents.[21] In selected instances, the radical anion can be formed in the presence of ether solvents. In each of these examples that we found, strong metal−ligand electronic interactions were invoked.[13−15] In a similar vein, we have previously observed that strong coupling between anion radical IP ligands through an aluminum center prevents C−C coupling of IP radicals of adjacent complexes to yield a dimer.[4] To our knowledge, deprotonation of ^{Me}IP ligands to form ^{CH2}IP complexes in a nonether solvent has not been observed, and thus ether solvents appear to be a key feature of ^{CH2}IP formation.

When complexes of the intact anion radical ligands are exposed to a strong base or to excess reducing agent, deprotonation to yield the $^{CH2}IP_{Mes}^{-}$ form of the ligand can again be observed. Recently Gambarotta and co-workers have shown that ($^{Me}I_2P^{-}$)CoCl can be deprotonated by NaH in THF under argon, although the same reaction run under an atmosphere of dinitrogen leads to coordination of a bridging N_2^{2-} ligand and no deprotonation.[14] In a subsequent report, ($^{Me}I_2P$)$FeCl_2$ underwent both reduction and deprotonation in THF under an N_2 atmosphere when exposed to either Na or NaH.[15] Given the precedent for deprotonation of the IP ligand class by strong bases we speculate that the role of the ether solvent in deprotonation of $^{Me}IP_{Mes}$ is to modify the basicity of the sodium metal that we employ for ligand reduction. That is, in noncoordinating benzene or toluene solvents sodium acts as a reductant only, and in ethereal solvents sodium behaves as both a reductant and a base.

Syntheses of aluminum complexes in which the $^{Me}IP_{Mes}$ ligand is reduced by two electrons were attempted by employing 2 equiv of sodium metal in conjunction with $^{Me}IP_{Mes}$ and MX_3 starting reagents (M = Al, Ga; X = Cl or Me, Scheme 1). Initial attempts in this endeavor were unsuccessful when ($^{Me}IP_{Mes}^{2-}$)AlCl or ($^{Me}IP_{Mes}^{2-}$)AlMe were targeted in nonether solvents. Preparation of deep purple, two-electron reduced complexes was successfully achieved when ether was employed to stabilize four coordinate complexes ($^{Me}IP_{Mes}^{2-}$)$AlCl(OEt_2)$ (**3**), ($^{Me}IP_{Mes}^{2-}$)$AlMe(OEt_2)$ (**4**) and ($^{Me}IP_{Mes}^{2-}$)$GaCl(OEt_2)$ (**6**). To prevent deprotonation of $^{Me}IP_{Mes}^{-}$ in diethylether, $^{Me}IP_{Mes}$ was allowed to complex to the metal salt, $AlCl_3$, $AlMe_3$, or $GaCl_3$, in ether before reduction by sodium metal. Under these conditions no alkene resonances were observed in the ^{1}H NMR spectrum of both the reaction mixture and the isolated product. Similar stabilization by coordination of ether has been previously observed for aluminum complexes of redox active dpp-BIAN ligands (dpp-BIAN = 1,2-bis[(2,6-diisopropyl phenyl)imino]-acenaphthene).[22]

Compounds **1**−**6** are soluble in alkane, aromatic, and ether solvents. The ^{1}H NMR spectra for the one-electron reduced and paramagnetic complexes of the $^{Me}IP_{Mes}^{-}$ ligand **1**, **2**, and **5** display proton resonances that are shifted from the expected positions and very broad. However, all resonances do occur between −1 and 11 ppm. For example, proton resonances corresponding to the pyridine rings fall in the range 7.25−6.40 ppm. Three methyl resonances are observed; one each for the methyl group on the imine carbon, the *o*-mesityl carbon atoms, and the *p*-mesityl carbon atom: 2.19, 2.11, and 2.02 ppm, respectively. The ^{1}H NMR spectra of the diamagnetic complexes, **3** and **4**, further support the assignment of the redox events as ligand-based. The observed chemical shifts corresponding to proton resonances on the pyridine ligands do not fall within the expected range of aromatic proton resonances because the pyridine ring is dearomatized upon two-electron reduction of $^{Me}IP_{Mes}$. For example, in **3** the protons corresponding to the dearomatized pyridine group of $^{Me}IP_{Mes}^{2-}$ are observed in the range 6.18−4.90 ppm.

Electronic Structure. We have previously reported that aluminum complexes of the IP^{-} and IP^{2-} are deep green and deep purple, respectively.[1] In the present work we have observed the same colors for complexes of the equivalent oxidation states of the $^{Me}IP_{Mes}^{-}$ and $^{Me}IP_{Mes}^{2-}$ ligands. The intense absorption bands responsible for these colors are assigned as ligand-based $\pi-\pi^*$ transitions (Supporting Information, Figure S1).

Magnetic susceptibility measurements were performed on complexes **1**−**4** (Supporting Information, Figure S2). Data was collected in an applied field of 1000 Oe between 4 and 300 K. Measurements were performed on multiple batches of sample and gave consistent results. Complexes **1**, **2**, and **5**, containing the $^{Me}IP_{Mes}^{-}$ ligand are paramagnetic with temperature

dx.doi.org/10.1021/ic201729b | *Inorg. Chem.* 2012, 51, 1480−1488

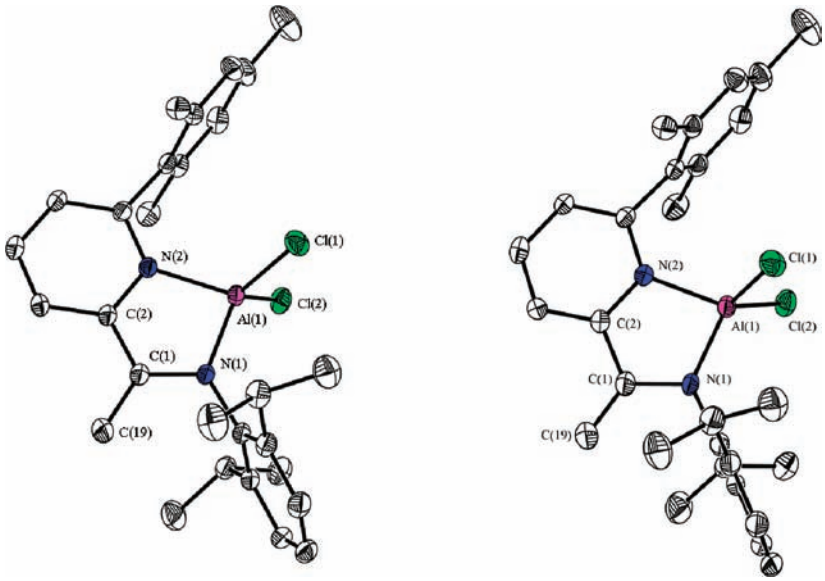

Figure 2. Structures of **1**, and **1a**. Pink, white, green, and blue ellipsoids represent Al, C, Cl, and N atoms ,respectively; ellipsoids are shown at the 50% probability level. H atoms omitted.

independent magnetic moments between 5−300 K consistent with one unpaired electron per complex; 1.73, 1.66, and 1.68 μ_B, respectively. As expected, complexes **3**, **4**, and **6**, which incorporate $^{Me}IP_{Mes}{}^{2-}$, are diamagnetic.

Solid State Structures of 1−7. Single crystals of compounds containing the one-electron reduced ligand, **1**, **2**, and **5**, were grown by chilling concentrated solutions of the complexes in hexanes at −25 °C for between 1 and 5 days each (Figures 2, 3, and Supporting Information, Figure S3). Compounds **3**, **4**,

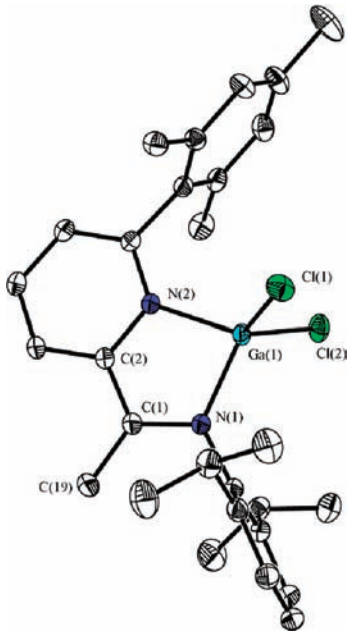

Figure 3. Structure of **5**. Light blue, white, green, and blue ellipsoids represent Ga, C, Cl, and N atoms, respectively; ellipsoids are shown at the 50% probability level. H atoms omitted.

and **7** which each incorporate two-electron reduced $^{Me}IP_{Mes}$ ligands were crystallized by chilling concentrated ether solutions at −25 °C for approximately 1 day. (Figures 4, 1, and Supporting Information, Figure S4) Each of the complexes are

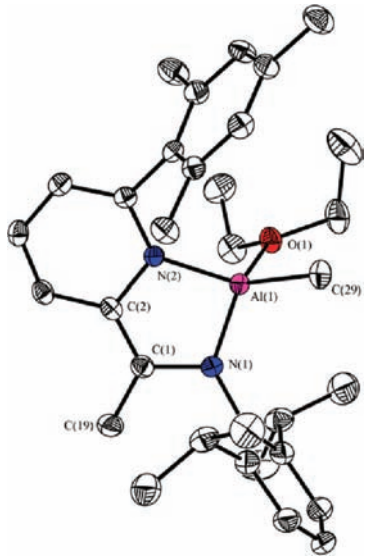

Figure 4. Structure of **4**. Pink, white, and blue ellipsoids represent Al, C, and N atoms, respectively; ellipsoids are shown at the 50% probability level. H atoms omitted.

four-coordinate with a pseudo tetrahedral geometry and contain one bidentate $^{Me}IP_{Mes}$ ligand and two monodentate ligands (Tables 1−3). In each of the tetrahedral complexes the bite angle of the bidentate, substituted iminopyridine ligand is less than the tetrahedral angle, 109.4°; in the one-electron reduced ligands this angle ranges from 83.92(7)° up to 87.24(6)° and in the two-electron reduced complexes the bite angle is slightly greater and falls between 89.17(8)° and 90.99(6)°. Similar bite angles were observed in the aluminum complexes of the unsubstituted IP ligands which we have previously reported.[4] In all of the complexes, the largest L−M−L angles are between the IP-based N_{im}/N_{py} atoms and the monodentate ligands, and these angles range from 113.96(4)° up to 127.49(5)°. X−M−X angles between monodentate ligands are in general quite close to tetrahedral and range from 102.86(4)° up to 115.42(9)°.

dx.doi.org/10.1021/ic201729b | *Inorg. Chem.* 2012, 51, 1480−1488

Table 1. Crystallographic Data[a] for the Complexes 1−2

	1	1a	2	2a
formula	C_{34} $H_{48}AlCl_2N_2$	$C_{34}H_{46}AlCl_2N_2$	$C_{33}H_{47}AlN_2$	$C_{36}H_{53}AlN_2$
crystal size	0.34 × 0.27 × 0.20	0.23 × 0.19 × 0.14	0.42 × 0.34 × 0.26	0.15 × 0.14 × 0.08
formula weight, g mol^{-1}	578.83	578.97	498.71	540.78
space group	$P2_1/c$	$P2_1/c$	$P2_1/c$	$P2_1/n$
a, Å	13.7327(4)	13.6859(11)	11.2859(4)	13.7281(4)
b, Å	17.9380(5)	17.9072(14)	17.0176(6)	17.9194(5)
c, Å	17.3440(4)	17.3368(10)	16.6324(6)	13.8370(4)
α, deg	90	90	90	90
β, deg	128.569(2)	128.517(4)	105.2380(10)	100.6650(10)
γ, deg	90	90	90	90
V, Å^3	3340.5(2)	3324.4(2)	3082.1(2)	3345.09(2)
Z	4	4	4	4
T, K	90(2)	90(2)	90(2)	90(2)
ρ, calcd, g cm^{-3}	1.151	1.157	1.075	1.074
refl. collected/$2\theta_{max}$	50732/66.52	40831/60.26	46498/64.70	44272/136.86
unique refl./ $I > 2\sigma$ (I)	12242/8607	9533/5097	10916/8185	5890/5598
no. parameters/restraints	372	383	336	352
λ, Å/μ (Kα), cm^{-1}	0.71073	0.71073	0.71073	1.54178
R1/GOF[b]	0.0519/1.042	0.0591/1.000	0.0542/0.943	0.0630/1.042
wR2 $(I > 2\sigma(I))^b$	0.1340	0.1370	0.1385	0.1817
residual density, e Å^{-3}	0.825/−0.786	0.483/−0.499	0.795/−0.563	1.045/−0.397

[a]Obtained with graphite-monochromated Mo Kα (λ = 0.71073 Å) radiation. [b]$R_1 = \sum||F_o| - |F_c||/\sum|F_o|$, $wR_2 = \{\sum w(F_o^2 - F_c^2)^2/\sum w(F_o^2)^2\}^{1/2}$.

Table 2. Crystallographic Data[a] for the Complexes 3, 4, 5, and 7

	3	4	5	7
formula	$C_{32}H_{44}AlClN_2O$	$C_{33}H_{47}AlON_2$	$C_{34}H_{48}Cl_2$ GaN_2	$C_{36}H_{53}N_2NaO_2$
crystal size	0.23 × 0.18 × 0.14	0.16 × 0.15 × 0.09	0.53 × 0.34 × 0.32	0.23 × 0.19 × 0.15
formula weight, g mol^{-1}	535.12	511.55	627.35	568.79
space group	$P2_1/c$	$P2_1/n$	$P2_1/n$	$Pbca$
a, Å	13.418(3)	13.680(3)	13.7380(12)	18.5932(5)
b, Å	15.976(3)	15.860(3)	17.9556(15)	16.5947(4)
c, Å	16.537(6)	14.630(3)	13.8993(12)	22.1689(6)
α, deg	90	90	90	90
β, deg	121.93(2)	108.94(3)	102.2780(10)	90
γ, deg	90	90	90	90
V, Å^3	3008.6(2)	3002.3(3)	3350.2(2)	6840.2(3)
Z	4	4	4	8
T, K	90(2)	90(2)	90(2)	90(2)
ρ, calcd, g cm^{-3}	1.181	1.132	1.240	1.105
refl. collected/$2\theta_{max}$	18915/50.74	11253/85.00	48679/65.20	83033/58.30
unique refl./ $I > 2\sigma(I)$	5437/4966	5347/4819	11482/10125	9216/8057
no. parameters/restraints	344	334	376	378
λ, Å/μ (Kα), cm^{-1}	0.71073	0.71073	0.71073	0.7107
R1/GOF[b]	0.0411/1.040	0.0553/1.040	0.0333/0.864	0.0402/1.040
wR2 $(I > 2\sigma(I))^b$	0.1081	0.1508	0.0921	0.1117
residual density, e Å^{-3}	0.437/−0.293	0.578/−0.355	0.763/−0.781	0.434/−0.351

[a]Obtained with graphite-monochromated Mo Kα (λ = 0.71073 Å) radiation. [b]$R_1 = \sum||F_o| - |F_c||/\sum|F_o|$, $wR_2 = \{\sum w(F_o^2 - F_c^2)^2/\sum w(F_o^2)^2\}^{1/2}$.

The bond lengths which are observed in complexes of the one-electron reduced $^{Me}IP_{Mes}$ ligand **1**, **2**, and **5** support assignment of the ligand oxidation state as −1 (Chart 1, Table 3). The Al−N_{im} bonds are 1.856(1) Å, 1.906(1) Å, and 1.907(1) Å respectively, which are even shorter than the Al−N_{im} bonds which we observed in one-electron reduced complexes of aluminum with the unsubsituted IP ligand (Table 4).[4] Evidence for the partial localization of the reduction event on the imine functionality was observed in the lengthening of the C=N double bonds to 1.370(2) Å, 1.362(2) Å, and 1.364(2) Å, respectively. The bond length trends for the C_{im}−C_{py} and C_{im}−C_{Me} bond lengths are also consistent with the 1− oxidation state (Chart 1). This is apparent when the bond lengths are compared with the neutral ligand complex (IP)$AlCl_3$ which we have previously reported. The C_{im}−C_{py} bond lengths for **1**, **2**, and **7** shorten a little at 1.435(2), 1.430(2), and 1.436(2) Å, respectively. These metrics are not as short as we have previously observed in IP^- complexes of aluminum (1.405(6) Å), but they are shorter than others have previously observed in complexes containing the neutral $^{Me}IP_{Mes}$ ligand (1.452(6) Å).[5,6] The C_{im}−C_{Me} bond lengths remain consistent with single bond character at 1.458(2), 1.459(2), and 1.462(2) Å, respectively. In each of these

dx.doi.org/10.1021/ic201729b | Inorg. Chem. 2012, 51, 1480−1488

Table 3. Selected Average Interatomic Distances (Å) and Selected Average Angles (deg) in 1−5 and 7

	(IP)$AlCl_3$[1]	1	1a	2	2a	3	4	5	7
M−N_{im}	1.856(1)	1.856(1)	1.828(3)	1.906(1)	1.871(2)	1.806(1)	1.828(2)	1.907(1)	2.3346(9)
M−N_{py}	1.909(1)	1.909(1)	1.923(3)	1.963(1)	1.988(2)	1.824(2)	1.847(2)	1.954(1)	2.4305(9)
M−X	2.1176(6)	2.1176(6)	2.116(1)	1.984(1)	1.969(2)	2.115(1)	1.938(3)	2.1605(4)	n/a
M−O	n/a	n/a	n/a	n/a	n/a	1.880(1)	1.935(2)	n/a	2.4417(9)
C_{im}−N_{im}	1.370(2)	1.370(2)	1.386(4)	1.362(2)	1.379(2)	1.425(2)	1.422(3)	1.364(2)	1.353(1)
C_{im}−C_{py}	1.435(2)	1.435(2)	1.474(4)	1.430(2)	1.492(3)	1.366(2)	1.366(3)	1.436(2)	1.501(1)
C_{py}−N_{py}	1.384(2)	1.384(2)	1.369(4)	1.383(2)	1.360(3)	1.390(2)	1.380(3)	1.364(2)	1.351(1)
C_{im}−C_{Me}	1.458(2)	1.458(2)	1.380(4)	1.459(2)	1.348(3)	1.494(2)	1.494(3)	1.462(2)	1.381(1)
N_{im}−M−N_{py}	87.24(6)	87.24(6)	87.1(1)	84.31(5)	83.92(7)	90.99(6)	89.17(8)	85.87(5)	70.18(3)
N_{py}−M−X	114.90(5)	114.90(5)	114.20(9)	116.38(5)	111.59(8)	127.49(5)	126.8(1)	115.29(4)	149.39(3)
N_{im}−M−X	113.96(4)	113.96(4)	115.31(9)	114.86(5)	114.90(7)	117.78(5)	123.0(1)	114.58(4)	126.96(3)
X−M−X	109.73(3)	109.73(3)	109.42(5)	113.44(6)	115.42(9)	n/a	n/a	109.68(2)	104.68(3)
N_{py}−M−O	n/a	n/a	n/a	n/a	n/a	106.04(6)	102.75(8)	n/a	97.59(3)
N_{im}−M−O	n/a	n/a	n/a	n/a	n/a	111.05(6)	107.90(8)	n/a	110.35(3)
X−M−O	n/a	n/a	n/a	n/a	n/a	102.86(4)	104.8(1)	n/a	104.68(3)
C_{py}−C_{im}−N_{im}	114.7(1)	114.7(1)	113.2(1)	115.16(9)	111.8(2)	119.2(1)	115.1(2)	115.6(1)	117.90(8)

Table 4. Comparison of Ligand Backbone Bond Lengths for One-Electron and Two-Electron Reduced Ligands from This Work with Values Reported in the Literature

		literature (Å)[1,8,20]	current work (Å)
$^{CH2}IP_{Mes}{}^{-}$ [a]	C_{im}−C_{py}	1.474(3)	1.483(4)
	C_{im}−N_{Im}	1.370(4)	1.382(4)
	C_{im}−C_{CH2}	1.309(3)	1.364(3)
	N_{Im}−Al	1.874(2)	1.850(3)
	N_{Py}−Al	1.953(2)	1.955(2)
$^{Me}IPMes^{-}$ [b]	C_{im}−C_{py}	1.435(3)	1.433(2)
	C_{im}−N_{im}	1.322(3)	1.366(2)
	C_{im}−C_{Me}	1.492(3)	1.458(2)
	N_{Im}−Al	1.915(1)	1.881(2)
	N_{Py}−Al	2.009(2)	1.936(2)
$^{Me}IPMes^{2-}$ [c]	C_{im}−C_{py}	1.356(6)	1.366(3)
	C_{im}−N_{im}	1.414(6)	1.423(3)
	C_{im}−C_{Me}	n/a	1.494(2)
	N_{Im}−Al	1.844(4)	1.817(2)
	N_{Py}−Al	1.873(4)	1.836(2)

[a]Average bond distances taken from **1a** and **2a**. [b]Average bond distances taken from **1** and **2**. Literature values for C_{im}−C_{py}, C_{im}−N_{im}, and C_{im}−C_{me} taken from $^{Me}I_2P^{-}$, values for N_{im}−Al and N_{py}−Al taken from IP^{-}. [c]Average bond distances taken from **3** and **4**. Literature values from IP^{2-}.

three one-electron reduced complexes the pyridine rings largely retain their aromatic character.

Complexes **1a** and **2a**, which were obtained when the reaction solvent is ether, display bond lengths and angles consistent with the $^{CH2}IP_{Mes}{}^{-}$ formulation for the reduced ligand (Chart 1, Table 3). Notable differences in the bond lengths described for the $^{Me}IP_{Mes}{}^{-}$ ligand in **1**, **2**, and **5** are observed for the C_{im}−N_{im}, C_{im}−C_{py}, and C_{im}−C_{Me} bonds. The C_{im}−C_{py} bond lengths do not exhibit structural changes consistent with the shortening of the C−C single bond. Instead, apparent shortening of the C_{im}−C_{Me} bond is observed, and these C_{im}−C_{Me} bonds are consistent with double bond character, at 1.380(4) Å and 1.348(3) Å, respectively. The C_{im}−C_{py} bond lengths are 1.474(4) and 1.492(3) Å. The C_{im}−N_{im} bonds lengthen more than was expected for the $^{Me}IP_{Mes}{}^{-}$ formulation of the ligand. At 1.386(4) and 1.379(2) Å, respectively, these bond lengths are also consistent with $^{CH2}IP_{Mes}{}^{-}$.

The bond lengths associated with complexes **3** and **4**, which contain the two-electron reduced $^{Me}IP_{Mes}{}^{2-}$ ligand, are characteristic of the IP^{2-} oxidation state that we and others have previously reported.[1,23] The foregoing discussion focuses on **3** only, because metrics for **4** are similar (Table 3). In accord with the higher negative charge on the ligand, the Al−N_{im} and Al−N_{py} bond lengths are both significantly shortened to 1.806(1) Å and 1.824(2) Å, respectively. The formerly C═N double bond is lengthened even further than observed in complex **1** and is 1.425(2) Å. The C_{im}−C_{py} bond length in this case is shortened as would be expected, and measures 1.366(2) Å. In further agreement with the two-electron reduced nature of the ligand, the pyridine ring is dearomatized and displays alternating bond lengths that approach the lengths expected in pure single and double bonds. The C_{im}−C_{Me} bond has a distance of 1.494(2) Å consistent with single bond character. Complex **4**, which incorporates a methyl monodentate ligand instead of the chloro monodentate ligand in **3**, displays the same general trends in bond length changes for the two-electron reduced state of $^{Me}IP_{Mes}$. However, these bond length changes are not as pronounced as we observed in **3**. The gallium analogue of these complexes, compound **6**, is diamagnetic and was identified by ^{1}H NMR and other spectroscopic techniques. We have no crystallographic data for this complex.

The sodium salt of the $^{CH2}IP_{Mes}{}^{-}$ ligand (**7**) displays bond distances and angles very similar to those we report for **1a** and **2a**. The C_{im}−C_{py} bond has lengthened to full single bond character at 1.501(1) Å. Additionally, the dihedral angle between the C_{im}−N_{im} and C_{py}−N_{py} bonds is 19.4(1)° indicating that pyridine and imine π systems are no longer in conjugation; this is also consistent with full C_{im}−C_{py} single bond character. Both the C_{im}−N_{im} and the C_{im}−C_{Me} bonds are between single and double bond character at 1.353(1) Å and 1.381(1) Å, respectively. These distances suggest that the negative charge is delocalized over C_{im}, N_{im}, and C_{Me} but not over the pyridine ring. The complex also has severe distortions away from an ideal tetrahedral geometry with N_{py}−Al−O angles of 97.59(3)° and 149.39(3)°.

Electrochemical Measurements. Cyclic voltammetry measurements were performed in 0.3 M Bu_4NPF_6 THF solutions of complexes **1**−**6** (Figure 5 and Supporting Information, Figure S5). For each of the complexes containing the one-electron reduced ligand, **1**, **2**, and **5**, the cyclic voltammogram

dx.doi.org/10.1021/ic201729b | Inorg. Chem. 2012, 51, 1480−1488

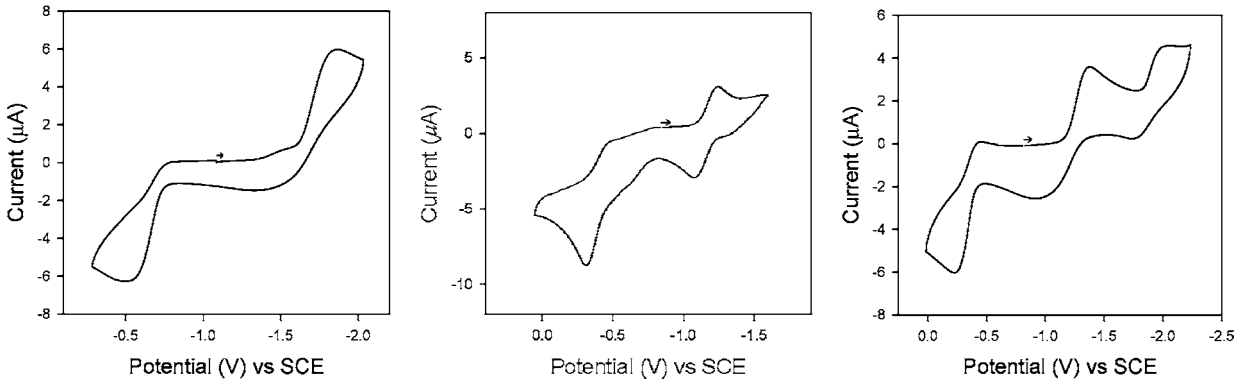

Figure 5. CVs for the complexes containing the one-electron reduced ligand, $^{Me}IP_{Mes}{}^{-}$: **1**, **2**, and **5**. Recorded in 0.3 M Bu_4NPF_6 THF solution.

(CV) displays one irreversible oxidation wave for the $^{Me}IP_{Mes}{}^{1-/0}$ couple and one reduction wave for the $^{Me}IP_{Mes}{}^{2-/1-}$ redox couple (Figure 5). The $^{Me}IP_{Mes}{}^{2-/1-}$ redox couple is reversible for complex **4** and irreversible for complexes **3** and **5**. Comparison of the CVs for **1** and **2** reveals that the redox couples for complex **4** are in general about 0.5 V more positive than those for complex **3** which suggests that the methyl substituted complex is more easily reduced. The CVs for the two-electron reduced complexes, **3**, **4**, and **6**, are significantly less well-defined than those for the one-electron reduced complexes (Supporting Information, Figure S5). The aluminum complexes **3** and **4** display no definitive redox activity, and the gallium complex, **6**, reveals two very broad and irreversible oxidation waves at −1.2 and +0.2 V vs SCE. Both of the broad oxidation events associated with **6** occur within 0.5 V of the corresponding redox couples observed for the one-electron reduced complex **5**.

Conclusions and Outlook. We have demonstrated that a bulky mesityl-substituted iminopyridine ligand ($^{Me}IP_{Mes}$) can be employed as a noninnocent ligand in a −1 or −2 oxidation state for aluminum(III) and gallium(III). Complexes of the monoanionic radical and dianionic $^{Me}IP_{Mes}$ ligand have been isolated for aluminum(IIII) and gallium(III), and their solid state structures demonstrate that the bulky ligand directs the formation of a complex with a single $^{Me}IP_{Mes}$ ligand. This is in contrast to the $[IP_2Al]$ formulation which we have consistently observed with the smaller IP ligand.[4] The solvent dependence we have observed for formation of complexes containing the one-electron reduced oxidation state of $^{Me}IP_{Mes}$, demonstrates that by controlling reactions conditions, especially solvent choice, the formation of the ligand $^{CH2}IP_{Mes}$ which involves loss of a hydrogen atom, can be avoided. This synthetic control will facilitate the exploration of the *reversible* redox processes that we wish to exploit. Future work will focus on the synthesis of cationic complexes and three-coordinate complexes of aluminum and gallium supported by the $^{Me}IP_{Mes}$ ligand. In addition, complexes analogous to **3** which utilize more weakly coordinating ligands than ether are being investigated.

EXPERIMENTAL SECTION

Physical Measurements. Elemental analyses were performed by Columbia Analytical. ^{1}H NMR spectra were recorded at ambient temperature using a Varian 400 MHz spectrometer. ^{1}H NMR spectra of all paramagnetic compounds were recorded from −80 ppm to 150 ppm. Chemical shifts were referenced to residual solvent. Electrochemical measurements were recorded in a glovebox under a dinitrogen atmosphere using a CH Instruments Electrochemical Analyzer, a glassy carbon working electrode, a platinum wire auxiliary-electrode, and an $Ag/AgNO_3$ nonaqueous reference electrode. Reported potentials are all referenced to the SCE couple, and were determined using decamethylferrocene as an internal standard. The number of electrons passed in a given redox process was estimated by comparison of the peak current with the peak current of decamethylferrocene included as an internal standard. UV−vis spectra were recorded in THF or hexane solutions using a Varian Cary 1 UV−vis spectrometer. Magnetic measurements were recorded using a Quantum Design MPMS XL magnetometer at 0.1 T. The sample was contained under nitrogen in a gelcap and suspended in the magnetometer in a plastic straw. The magnetic susceptibility was adjusted for diamagnetic contributions using the constitutive corrections of Pascal's constants.

X-ray Structure Determinations. X-ray diffraction studies were carried out on a Bruker SMART 1000, a Bruker SMART APEXII, or a Bruker SMART APEX Duo diffractometer equipped with a CCD detector.[24] Measurements were carried out at −175 °C using Mo Kα (λ = 0.71073 Å) and Cu Kα (1.5418 Å) radiation. Crystals were mounted on a glass capillary or Kaptan Loop with Paratone-N oil. Initial lattice parameters were obtained from a least-squares analysis of more than 100 centered reflections; these parameters were later refined against all data. Data were integrated and corrected for Lorentz polarization effects using SAINT and were corrected for absorption effects using SADABS2.3.

Space group assignments were based upon systematic absences, *E* statistics, and successful refinement of the structures. Structures were solved by direct methods with the aid of successive difference Fourier maps and were refined against all data using the SHELXTL 5.0 software package. Thermal parameters for all non-hydrogen atoms were refined anisotropically. Hydrogen atoms, where added, were assigned to ideal positions and refined using a riding model with an isotropic thermal parameter 1.2 times that of the attached carbon atom (1.5 times for methyl hydrogens).

Preparation of Compounds. All manipulations were carried out using standard Schlenk or glovebox techniques under a dinitrogen atmosphere. Unless otherwise noted, solvents were deoxygenated and dried by thorough sparging with Ar gas followed by passage through an activated alumina column. Deuterated solvents were purchased from Cambridge Isotopes Laboratories, Inc. and were degassed and stored over activated 3 Å molecular sieves prior to use. The ligand $^{Me}IP_{Mes}$ was prepared according to literature procedures.[25] All other reagents were purchased from commercial vendors and used without further purification.

($^{Me}IP_{Mes}{}^{-}$)$AlCl_2$ (1). To a solution of $^{Me}IP_{Mes}$ (500 mg, 1.26 mmol) in benzene (15 mL) was added sodium (29.1 mg, 1.26 mmol). The yellow solution was stirred for 4 h until all the sodium was consumed and the solution was a dark red color. To this solution aluminum trichloride (168 mg, 1.26 mmol) was added in portions to yield a dark green solution and a gray precipitate. The reaction mixture was stirred overnight. The resulting dark green solution was evaporated to dryness, extracted into hexane (20 mL), and filtered through Celite to remove salts. The green filtrate was concentrated to 10 mL and cooled at −25 °C overnight to yield a dark green powder (343 mg, 70%). Single crystals suitable for X-ray diffraction were grown by cooling a

dx.doi.org/10.1021/ic201729b | *Inorg. Chem.* 2012, 51, 1480−1488

concentrated hexane solution to −25 °C overnight. ^{1}H NMR (300 MHz, C_6D_6) δ 7.44 (br), 5.85 (br), 4.47 (br), 4.27 (br), 3.41 (br), 2.76 (br), 2.63 (br) ppm. IR (KBr): 3054 (m), 2968 (vs), 2930(vs), 2869 (s), 1614 (s) 1573 (s), 1534 (m), 1510 (m), 1465 (vs), 1445 (vs), 1385 (s), 1353 (s), 1324 (s), 1281 (s), 1267 (s), 852 (s), 762 (s), 731 (s), 703 (s), 662 (s), 535 (vs), 495 (vs) cm^{-1}. UV−vis spectrum (Hexane) λ_{max} (ε_M): 267 (29 590), 370 (32 180), 402 (16 940), 440 (8760), 738 (1640) nm (L mol^{-1} cm^{-1}). Anal. Calcd. For $C_{28}H_{35}N_2AlCl_2$: C, 67.74; H, 6.90; N, 5.64. Found C, 67.92; H, 7.01; N, 5.57. μ_{eff} = 1.73 μ_B.

(^{CH2}IP$_{Mes}^-$)AlCl$_2$ (1a). To a solution of ^{Me}IP$_{Mes}$ (500 mg, 1.26 mmol) in ether (15 mL) was added sodium (29.1 mg, 1.27 mmol). The yellow solution was stirred for 4 h until all the sodium was consumed and the solution was a dark red color. To this solution aluminum trichloride (169 mg, 1.26 mmol) was added in portions to afford a dark green solution and a gray precipitate. The reaction mixture was stirred overnight. The resulting dark green solution was evaporated to dryness, extracted into hexane (20 mL), and filtered through Celite to remove salts. The green filtrate was concentrated to 10 mL and cooled at −25 °C overnight to afford a dark green powder (357 mg, 72%). Single crystals suitable for X-ray diffraction were grown by cooling a concentrated hexane solution to −25 °C overnight. ^{1}H NMR (300 MHz, C_6D_6) δ 7.30 (d, J = 7.42, 2H, py), 7.25 (s, 2H, Mes), 6.90 (m, 1H, ph), 6.83 (d, J = 7.42, 2H, ph), 6.47 (t, J = 8.53, 1H, py), 6.40 (d, J = 8.53, 1H, py), 4.73 (d, J = 7.66, 1H, im CH_2), 4.03 (d, J = 7.66, 1H, im CH_2), 3.62 (sept, J = 7.43, 2H, CH(CH$_3$)$_2$), 2.08 (s, 3H, Mes), 2.02 (s, 6H, Mes), 1.29 (d, J = 7.42, 12H, CH(CH$_3$)$_2$) ppm.

(^{Me}IP$_{Mes}^-$)AlMe$_2$ (2). To a solution of ^{Me}IP$_{Mes}$ (500 mg, 1.26 mmol) in benzene (15 mL) was added sodium (29.1 mg, 1.27 mmol). The yellow solution was stirred for 4 h until all the sodium was consumed and the solution was a dark red color. Carefully in portions dimethyl aluminum chloride (1.26 mL, 1 M in hexane, 1.26 mmol) was added, and a dark green solution and a gray precipitate was obtained. The reaction mixture was stirred overnight. The resulting dark green solution was evaporated to dryness, extracted into hexane (20 mL) and filtered through Celite to remove salts. The green filtrate was concentrated to 10 mL and cooled at −25 °C overnight to afford a dark green powder (451 mg, 78%). Single crystals suitable for X-ray diffraction were grown by cooling a concentrated hexane solution to −25 °C for 3 days. ^{1}H NMR (300 MHz, C_6D_6) δ 7.61 (br), 5.83 (br), 4.41 (br), 4.25 (br), 3.37 (br), 3.07 (br), 2.20 (br), −1.84 (br) ppm. ppm. IR (KBr): 3060 (m), 2967 (vs), 2952 (vs), 2925 (vs), 2870 (s), 1615 (s), 1570 (s), 1531 (s), 1528 (s), 1451 (vs), 1397 (s), 1393 (s), 1377 (s), 1366 (s), 1321 (s), 970 (s), 795 (s), 760 (vs), 726 (s), 701 (s), 688 (s) cm^{-1}. UV−vis spectrum (Hexane) λ_{max} (ε_M): 375 (23 950), 427 (8430), 461 (6730), 750 (2310) nm (L mol^{-1} cm^{-1}). Anal. Calcd. For $C_{30}H_{39}N_2Al$: C, 79.08; H, 8.85; N, 6.15. Found C, 79.45; H, 8.89; N, 6.07. μ_{eff} = 1.66 μ_B.

(^{CH2}IP$_{Mes}^-$)AlMe$_2$ (2a). To a solution of ^{Me}IP$_{Mes}$ (500 mg, 1.26 mmol) in ether (15 mL) was added sodium (29.1 mg, 1.27 mmol). The yellow solution was stirred for 4 h until all the sodium was consumed and the solution was a dark red color. Dimethyl aluminum chloride (1.26 mL, 1 M in hexane, 1.26 mmol) was added in portions to yield a dark green solution and a gray precipitate. The reaction mixture was stirred overnight. The resulting dark green solution was evaporated to dryness, extracted into hexane (20 mL), and filtered through Celite to remove salts. The green filtrate was concentrated to 10 mL and cooled at −25 °C overnight to yield a dark green powder (421 mg, 74%). Single crystals suitable for X-ray diffraction were grown by cooling a concentrated hexane solution to −25 °C for 3 days. ^{1}H NMR (300 MHz, C_6D_6) δ 7.39 (d, J = 7.67, 1H, py), 7.29 (s, 2H, Mes), 6.88 (t, J = 7.67, 1H, ph), 6.76 (d, J = 7.44, 2H, ph), 6.57 (d, J = 8.62, 1H, py), 6.43 (t, J = 8.62, 1H, py), 4.68 (d, J = 7.56, 1H, im CH_2), 3.90 (d, J = 7.32, 1H, im CH_2), 3.62 (sept, J = 7.67, 2H, CH(CH$_3$)$_2$), 2.05 (s, 3H, Mes), 1.89 (s, 6H, Mes), 1.38 (d, J = 7.67, 12H, CH(CH$_3$)$_2$), −0.61 (s, 3H, Al−CH_3) ppm.

(^{Me}IP$_{Mes}^{2-}$)AlCl(OEt$_2$) (3). To a solution of ^{Me}IP$_{Mes}$ (500 mg, 1.26 mmol) in ether (20 mL) was added aluminum trichloride (169 mg, 1.26 mmol). The yellow solution was stirred for 30 min. Next sodium (72.7 mg, 3.16 mmol) was added to yield a dark green solution initially and a gray precipitate. The reaction mixture was stirred for 24 h until the solution turned purple. The solution was filtered through Celite to remove salts. The purple filtrate was concentrated to 10 mL and cooled at −25 °C overnight to afford a dark purple powder (424 mg, 63%). Single crystals suitable for X-ray diffraction were grown by cooling a concentrated ether solution to −25 °C for 3 h. ^{1}H NMR (300 MHz, C_6D_6) δ 7.20−7.14 (m, 3H, ph), 6.86 (s, 1H, Mes CH), 6.76 (s, 1H, Mes CH), 6.18 (d, J = 9.6, 1H, py), 5.79 (dd, J = 5.7, 9.7, 1H, py), 4.87 (d, J = 5.70, 1H, py), 3.59 (hept, J = 6.84, 1H, CH(CH$_3$)$_2$), 3.46 (q, J = 7.04, 2H, Ether CH_2), 3.41 (q, J = 7.04, 2H, Ether CH_2), 3.10 (sept, J = 6.84, 1H, CH(CH$_3$)$_2$), 2.74 (s, 3H, imCH_3), 2.35 (s, 3H, Mes p-CH_3), 2.17 (s, 3H, Mes o-CH_3), 1.71 (s, 3H, Mes o-CH_3), 1.44 (d, J = 6.9, 3H, CH(CH_3)$_2$), 1.32 (d, J = 6.8, CH(CH_3)$_2$), 1.24 (d, J = 6.9, 3H, CH(CH_3)$_2$), 1.04 (d, J = 7.0, 3H, CH(CH_3)$_2$), 0.65 (t, J = 7.04, 6H, Ether CH_3) ppm. IR (KBr): 3035 (m), 2961 (vs), 2973 (vs), 2926 (vs), 2867 (s), 1611 (m), 1577 (m), 1540 (m), 1463 (vs), 1441 (vs), 1381 (s), 1342 (s), 1324 (s), 1283 (vs), 1274 (vs), 1201 (s), 1154 (s), 1129 (s), 1101 (s), 1017 (s), 799 (s), 766 (vs), 734 (s), 682 (vs) cm^{-1}. UV−vis spectrum (THF) λ_{max} (ε_M): 250 (41 900), 322 (23 560), 385 (22 820), 463 (13 210), 744 (2860) nm (L mol^{-1} cm^{-1}). Anal. Calcd. For $C_{32}H_{44}N_2O_2AlCl$: C, 71.82; H, 8.29; N, 5.23. Found C, 72.03; H, 8.17; N, 5.46.

(^{Me}IP$_{Mes}^{2-}$)AlMe(OEt$_2$) (4). To a solution of ^{Me}IP$_{Mes}$ (500 mg, 1.26 mmol) in ether (20 mL) methyl aluminum dichloride (1.26 mL, 1 M in hexane, 1.26 mmol) was added in portions. The yellow solution was stirred for 30 min. Next sodium (72.7 mg, 3.16 mmol) was added to yield a dark green solution initially and a gray precipitate. The reaction mixture was stirred for 24 h until the solution turned purple. The solution was filtered through Celite to remove salts. The purple filtrate was concentrated to 10 mL and cooled at −25 °C overnight to yield a dark purple powder (380 mg, 59%). Single crystals suitable for X-ray diffraction were grown by cooling a concentrated ether solution to −25 °C for 3 h. ^{1}H NMR (300 MHz, C_6D_6) δ 7.17−7.24 (m, 3H, ph), 6.90 (s, 1H, Mes CH), 6.85 (s, 1H, Mes CH), 6.33 (d, J = 9.6, 1H, py), 5.96 (dd, J = 5.7, 9.7, 1H, py), 4.91 (d, J = 5.7, 1H, py), 4.36 (hept, J = 6.84, 1H, CH(CH$_3$)$_2$), 3.92 (sept, J = 6.84, 1H, CH(CH$_3$)$_2$), 3.39−3.49 (m, 4H, Ether CH_2), 2.77 (s, 3H, imCH_3), 2.40 (s, 3H, Mes p-CH_3), 2.23 (s, 3H, Mes o-CH_3), 1.85 (s, 3H, Mes o-CH_3), 1.42 (d, J = 6.9, 3H, CH(CH_3)$_2$), 1.34 (d, J = 6.8, CH(CH_3)$_2$), 1.30 (d, J = 6.9, 3H, CH(CH_3)$_2$), 1.12 (t, J = 7.04, 6H, Ether CH_3), 0.95 (d, J = 7.0, 3H, CH(CH_3)$_2$), −1.15 (s, 3H, Al−CH_3) ppm. IR (KBr): 3035 (m), 2961 (vs), 2973 (vs), 2926 (vs), 2867 (s), 1615 (m), 1572 (m), 1537 (m), 1463 (vs), 1441 (vs), 1381 (s), 1351 (s), 1323 (s), 1283 (vs), 1274 (vs), 1199 (s), 1154 (s), 1129 (s), 1101 (s), 795 (s), 760 (s), 733 (s), 704 (s), 663 (s), 587 (s) cm^{-1}. UV−vis spectrum (THF) λ_{max} (ε_M): 253 (40280), 337 (21900), 381 (24710), 451 (15650), 750 (3290) nm (L mol^{-1}cm^{-1}). Anal. Calcd. For $C_{33}H_{47}N_2O_2Al$: C, 77.00; H, 9.20; N, 5.44. Found C, 77.15; H, 9.24; N, 5.32.

(^{Me}IP$_{Mes}^-$)GaCl$_2$ (5). To a solution of ^{Me}IP$_{Mes}$ (500 mg, 1.26 mmol) in benzene (15 mL) was added sodium (29.1 mg, 1.27 mmol). The yellow solution was stirred for 4 h until all the sodium was consumed and the solution was a dark red color. To this solution gallium trichloride (222 mg, 1.26 mmol) was added in portions to yield a dark green solution and a gray precipitate. The reaction mixture was stirred overnight. The resulting dark green solution was evaporated to dryness, extracted into hexane (20 mL) and filtered through Celite to remove salts. The green filtrate was concentrated to 10 mL and cooled at −25 °C overnight to afford a dark green powder (365 mg, 68%). Single crystals suitable for X-ray diffraction were grown by cooling a concentrated hexane solution to −25 °C overnight. ^{1}H NMR (300 MHz, C_6D_6) δ 7.81 (br), 6.17 (br), 5.37 (br), 4.25 (br), 4.03 (br), 3.31 (br), 2.61 (br) ppm. IR (KBr): 3062 (m), 2963 (vs), 2925 (vs), 2870 (s), 2736 (w), 1642 (s), 1614 (s), 1582 (s), 1569 (vs), 1535 (s), 1505 (m), 1464 (vs), 1446 (vs), 1396 (vs), 1388 (vs), 1378 (s), 1363 (s), 1023 (s), 854 (s), 820 (s), 799 (s), 786 (s), 775 (vs) cm^{-1}. UV−vis spectrum (Hexane) λ_{max} (ε_M): 284 (26400), 370 (22610), 428 (11010), 737 (2930) nm (L mol^{-1}cm^{-1}). Anal. Calcd. C, 62.51; H, 6.36; N, 5.20. Found C, 62.26; H, 6.42; N, 5.07. μ_{eff} = 1.68 μ_B.

(^{Me}IP$_{Mes}^{2-}$)GaCl(OEt$_2$) (6). To a solution of ^{Me}IP$_{Mes}$ (500 mg, 1.26 mmol) in ether (20 mL) was added sodium (72.7 mg, 3.16 mmol). The yellow solution was stirred for 4 h until all the sodium was consumed and the solution was a dark brown color. To this solution gallium trichloride (221 mg, 1.26 mmol) was added in portions initially to afford a dark green solution and a gray precipitate. The reaction mixture was stirred for 24 h until the solution turned purple.

dx.doi.org/10.1021/ic201729b | Inorg. Chem. 2012, 51, 1480−1488

The solution was filtered through Celite to remove salts. The purple filtrate was concentrated to 10 mL and cooled at −25 °C overnight and a dark purple powder (407 mg, 61%) was obtained. ^{1}H NMR (300 MHz, C_6D_6) 7.24−7.31 (m, 2H, ph), 7.19 (s, 2H, Mes), 7.03 (t, J = 7.30, 1H, ph), 6.85 (s, 1H, Mes), 6.36 (t, J = 7.98, 1H, py), 4.74 (q, J =6.90, 1H, py), 4.39 (t, J =6.60, 1H, py), 3.67 (hept, J = 6.21, 2H, $CH(CH_3)_2$), 3.57 (m, 4H, Ether), 2.79 (hept, J = 6.21, 2H, $CH(CH_3)_2$), 2.31 (s, 3H, im-CH_3), 2.11 (s, 3H, Mes), 2.07 (s, 3H, Mes), 1.97 (s, 3H, Mes), 1.44 (d, J = 7.60, 3H, $CH(CH_3)_2$), 1.40 (d, J = 7.60, 3H, $CH(CH_3)_2$), 1.31 (d, J = 7.60, 3H, $CH(CH_3)_2$), 1.13 (d, J = 7.60, 3H, $CH(CH_3)_2$) ppm. IR (KBr): 3031 (m), 2968 (vs), 2975 (vs), 2926 (vs), 2865 (s), 2736 (w), 1610 (m), 1573 (m), 15380 (m), 1462 (vs), 1443 (vs), 1380 (s), 1342 (s), 1324 (s), 1281 (vs), 1272 (vs), 1198 (s), 1153 (s), 1132 (s), 1101 (s), 1018 (s), 854 (m), 799 (s), 767 (vs), 734 (s), 682 (vs), 606 (m), 550 (m), 538 (w), 521 (m), 438 (w) cm^{-1}. UV−vis spectrum (THF) λ_{max} (ε_M): 370 (15 580) nm (L mol^{-1}cm^{-1}). Anal. Calcd. C, 66.51; H 7.67; N, 4.85. Found C, 66.22; H, 8.02; N, 4.67.

(^{CH2}IP$_{Mes}^-$)Na(OEt$_2$)$_2$ (7). To a solution of ^{Me}IP$_{Mes}$ (200 mg, 0.51 mmol) in ether (5 mL) was added sodium (11.6 mg, 0.51 mmol). The yellow solution was stirred for 4 h until all the sodium was consumed and the solution was brown. The resulting solution was cooled overnight at −25 °C, and a brown powder (106 mg, 52%) was collected by filtration, washed with hexane (5 mL) and dried overnight. Single crystals suitable for X-ray diffraction were grown by cooling a concentrated ether solution to −25 °C overnight. ^{1}H NMR (300 MHz, C_6D_6) 7.41 (m, 1H, py), 7.31 (s, 2H, Mes), 7.03 (m, 1H, ph), 6.84 (m, 2H, pH), 6.63 (d, J = 8.54, 1H, py), 6.59 (t, J = 8.32, 1H, py), 4.22 (d, J = 7.22, 1H, im-CH_2), 3.53 (d, J = 7.13, 1H, im-CH_2), 3.38 (m, 2H, $CH(CH_3)_2$, 3.04 (m, 8H, ether), 2.10 (s, 3H, Mes), 1.88 (s, 6H, Mes), 1.25 (d, J = 7.45, 12H, $CH(CH_3)_2$), 0.89 (m, 12H, ether) ppm. Anal. Calcd. C, 76.02; H 9.39; N, 4.92. Found C, 76.16; H, 9.24; N, 4.77.

■ ASSOCIATED CONTENT

Ⓢ Supporting Information

CIF files for the structures of **1**−**7**. UV−vis spectra for **1**−**6**. Depictions of the solid state structures of **2**, **2a**, **3**, and **7**. CVs for **3**, **4**, and **6**. Plots of magnetic susceptibility data. This material is available free of charge via the Internet at http://pubs.acs.org.

■ AUTHOR INFORMATION

Corresponding Author

*E-mail: laberben@ucdavis.edu.

■ ACKNOWLEDGMENTS

We would like to thank the University of California Davis for funding and Drs. M. Shanmugam and J. C. Fettinger for experimental assistance.

■ REFERENCES

(1) Hameline, M. R.; Heyduk, A. H. *J. Am. Chem. Soc.* **2006**, *128*, 8410.

(2) (a) Westerhausen, M.; Bollwein, T.; Makropoulos, N.; Schneiderbauer, S.; Suter, S.; Nöth, H.; Mayer, P.; Piotrowski, H.; Polborn, K.; Pfitzner, A. *Eur. J. Inorg. Chem.* **2002**, 389. (b) Lu, C. C.; Bill, E.; Weyhermüller, T.; Bothe, E.; Wieghardt, K. *J. Am. Chem. Soc.* **2008**, *130*, 3181.

(3) Lu, C. C.; De Beer George, S.; Weyhermüller, T.; Bill, E.; Bothe, E.; Wieghardt, K. *Angew. Chem., Int. Ed.* **2008**, *47*, 1.

(4) (a) Myers, T. W.; Kazem, N.; Stoll, S.; Britt, R. D.; Shanmugam, M.; Berben, L. A. *J. Am. Chem. Soc.* **2011**, *133*, 8662. (b) Myers, T. W.; Berben, L. A. *J. Am. Chem. Soc.* **2011**, *133*, 11865.

(5) Hong, S.; Huber, S. M.; Gagliardi, L.; Cramer, C. C.; Tolman, W. B. *J. Am. Chem. Soc.* **2007**, *129*, 14190.

(6) Bianchini, C.; Mantovani, G.; Meli, A.; Migliacci, F. *Organometallics* **2003**, *22*, 2545.

(7) Kleigrewe, N.; Steffen, W.; Blömker, T.; Kehr, G.; Fröhlich, R.; Wibbeling, B.; Erker, G.; Wasilke, J.; Wu, G.; Bazan, Q. C. *J. Am. Chem. Soc.* **2005**, *127*, 13955.

(8) Kim, Y. H.; Kim, T. H.; Kim, N. Y.; Cho, E. S.; Lee, B. Y.; Shin, D. M.; Chung, Y. K. *Organometallics* **2003**, *22*, 1503.

(9) (a) Chen, Y.; Boardman, B. M.; Wu, G.; Bazan, G. C. *J. Organomet. Chem.* **2007**, *692*, 4745. (b) Kim, H. Y.; Kim, T. H.; Lee, B. Y. *Organometallics* **2002**, *21*, 3082.

(10) Wagler, J.; Bohme, U.; Brendler, E.; Thomas, B.; Goutal, S.; Mayr, H.; Kempf, B.; Remennikov, G. Y.; Roewer, G. *Inorg. Chim. Acta* **2005**, *358*, 4270.

(11) Porter, R. M.; Winston, S.; Danopoulos, A. A.; Hursthouse, M. B. *J. Chem. Soc., Dalton. Trans.* **2002**, 3290.

(12) Matthias, D.; Yao, S.; Brym, M.; Wullen, C. V. *Angew. Chem., Int. Ed.* **2006**, *45*, 4349.

(13) (a) Vidyaratne, I.; Gambarotta, S.; Korobkov, I.; Budzelaar, P. H. M. *Inorg. Chem.* **2005**, *44*, 1187. (b) deBruin, B.; Bill, E.; Bothe, E.; Weyhermüller, T.; Wieghardt, K. *Inorg. Chem.* **2000**, *39*, 2936.

(14) Sugirama, H.; Aharonian, G.; Gambarotta, S.; Yap, G. P. A; Budzelaar. *J. Am. Chem. Soc.* **2002**, *124*, 12268.

(15) Vidyaratne, I.; Scott, J.; Gambarotta, S.; Budzelaar, P. H. M. *Inorg. Chem.* **2007**, *46*, 7040.

(16) Scott, J.; Vidyaratne, I.; Korobkov, I.; Gambarotta, S.; Budzelaar, P. H. M. *Inorg. Chem.* **2008**, *47*, 896.

(17) Joung, U. G.; Kim, T. H.; Joe, D. J.; Lee, B. Y.; Shin, D. M.; Chung, Y. K. *Polyhedron* **2004**, *23*, 1587.

(18) (a) Sugiyama, H.; Korobkov, I.; Gambarotta, S. *Inorg. Chem.* **2004**, *43*, 5771. (b) Sugiyama, H.; Gambarotta, S.; Yap, G. P. A; Wilson, D. R.; Thiele, S. K. H. *Organometallics* **2004**, *23*, 5054. (c) Khorobkov, I.; Gambarotta, S.; Yap, G. P. A *Organometallics* **2002**, *21*, 3088.

(19) Scott, J.; Gambarotta, S.; Korobokov, I.; Knijnenburg, Q.; deBruin, B.; Budzelaar., P. H. M. *J. Am. Chem. Soc.* **2006**, *127*, 17204.

(20) Jurca, T.; Dawson, K.; Mallow, I.; Burchell, T.; Yap, G. P. A.; Richeson, D. S. *Dalton. Trans.* **2010**, *39*, 1266.

(21) Bowman, A. C.; Milsmann, C.; Atienza, C. C. H.; Lobkovsky, E.; Weighardt, K.; Chirik, P. J. *J. Am. Chem. Soc.* **2010**, *132*, 1676.

(22) Fedushkin, I. L.; Lukoyanov, A. N.; Hummert, M.; Schumann, H. *Z. Anorg. Allg. Chem.* **2008**, *634*, 356.

(23) Lu, C. C.; Weyhermüller, T.; Bill, E.; Wieghardt, K. *Inog. Chem.* **2009**, *48*, 6055.

(24) (a) *SMART Software Users Guide*, Version 5.1; Bruker Analytical X-Ray Systems, Inc.; Madison, WI, 1999. (b) *SAINT Software Users Guide*, Version 7.0; Bruker Analytical X-Ray Systems, Inc.: Madison, WI, 1999. (c) Sheldrick, G. M. *SADABS*, Version 2.03; Bruker Analytical X-Ray Systems, Inc.: Madison, WI, 2000. (d) Sheldrick, G. M. *SHELXTL*, Version 6.12; Bruker Analytical X-Ray Systems, Inc.: Madison, WI, 1999. (e) *International Tables for X-Ray Crystallography*; Kluwer Academic Publishers: Dordrecht, The Netherlands, 1992; Vol. *C*.

(25) Laine, T. V.; Klinga, M.; Leskelä, M. *Eur. J. Inorg. Chem.* **1999**, 959.